Molecular BioSystems

Accepted Manuscript

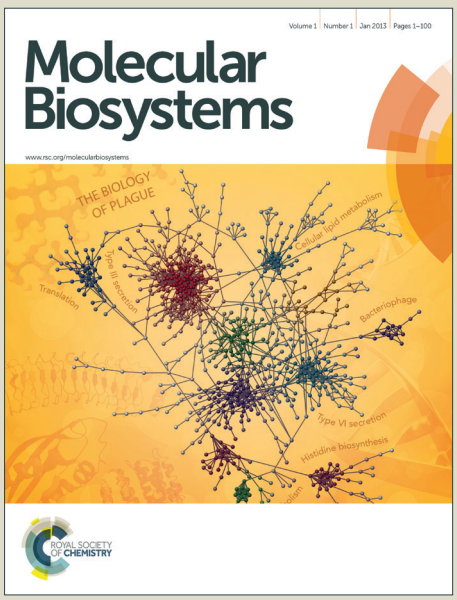

ROYAL SOCIETY OF CHEMISTRY

www.rsc.org/molecularbiosystems

Journal Name

RSCPublishing

ARTICLE

Grafting synthetic transmembrane units to the engineered low-toxicity α-hemolysin to restore its hemolytic activity

Cite this: DOI: 10.1039/x0xx00000x

Received 00th January 2012,
Accepted 00th January 2012

DOI: 10.1039/x0xx00000x

www.rsc.org/

Mihoko Ui,*[a] Kousuke Harima,[a] Toshiaki Takei,[b] Kouhei Tsumoto,[b, c, d] Kazuhito V. Tabata,[e] Hiroyuki Noji,[e] Sumire Endo,[a] Kimio Akiyama,[a] Takahiro Muraoka[a] and Kazushi Kinbara*[a]

The chemical modification of proteins to provide desirable functions and/or structures broadens their possibilities for use in various applications. Usually, proteins can acquire new functions and characteristics, in addition to their original ones, via the introduction of synthetic functional moieties. Here, we adopted a more radical approach to protein modification, *i.e.*, the replacement of a functional domain of proteins with alternative chemical compounds to build "cyborg proteins." As a proof of concept model, we chose staphylococcal α-hemolysin (Hla), which is a well-studied, pore-forming toxin. The hemolytic activity of Hla mutants was dramatically decreased by truncation of the stem domain, which forms a β-barrel pore in the membrane. However, the impaired hemolytic activity was significantly restored by attaching a pyrenyl-maleimide unit to the cysteine residue that was introduced in the remaining stem domain. In contrast, negatively charged fluorescein-maleimide completely abolished the remaining activity of the mutants.

Introduction

The chemical modification of proteins opens the way for their applications in various fields, including those of biology, medicine, and materials science.[1–4] A synthetic unit bearing a reactive group targeting a specific amino acid residue, such as cysteine or lysine, is introduced into the target protein via covalent-bond formation.[5–7] Recently, not only natural amino acids, but also unnatural amino acids have been used to label proteins.[8,9] The introduction of such an artificial moiety at the appropriate site allows the acquisition by the target protein of activities and/or structures that are suitable for the desired purpose and that are not necessarily related to its original biological functions.[10–15] These conventional strategies for protein modification inherently allow the synthetic functional moiety to diverge from the main chain. In this context, Lopez-Rodriguez *et al*. recently reported the replacement of amino acid side chains with synthetic moieties with chemical properties that were similar to those of the original side chain.[16]

Here, we propose a rather different approach to protein engineering compared with the conventional molecular design. First, a partial functional domain was cut off from the middle of the main chain of the target protein, so that its original function was mostly lost. Then, by introduction of synthetic prosthetic units at a specific site located close to the truncated part, the engineered protein recovered its original function. Namely, the original function of the peptide chain was complemented by synthetic moieties, to restore the original function. Such protein "cyborgs," in which the main chain of proteins is substituted with synthetic modules, would be advantageous to tune and control protein activity arbitrarily.

As a model protein for the present proof-of-concept study, we focused on a transmembrane protein. Typically, such proteins consist of three domains: an extracellular domain, a transmembrane domain, and an intracellular domain. Among them, the transmembrane domain often plays key roles in protein functions in addition to anchoring the protein in the membrane. Therefore, we expected that this domain would be suitable for replacement with synthetic hydrophobic moieties, so as to tune the original function according to the properties of the synthetic units. In the present study, we chose staphylococcal α-hemolysin (Hla).[17–19] Hla is a β-barrel, pore-forming toxin that binds to mammalian cells and forms a transmembrane pore via oligomerization at the cell membrane, to eventually cause lethal damage to cells. When expressed as a water-soluble monomer in aqueous solution, Hla assembles into a cyclic 7-mer at the susceptible cell membrane or synthetic lipid bilayers. After the formation of the 7-meric ring, the stem domain of Hla forms a β-barrel pore that penetrates the lipid bilayer of the cell. In the case of mammalian red blood cells, ions and water pass passively through the pore, causing hemolysis. In addition to its biological and clinical importance

as a bacterial toxin, Hla also presents an attractive framework for constructing nanopore devices for several biotechnological applications.[20,21]

In the present study, we constructed Hla mutants in which the stem domains were partially truncated to reduce or abolish hemolytic activity. Then, synthetic molecules were introduced at the site located close to the truncated stem domain. We found that the stem-truncated mutants restored Hla activity via the introduction of nonionic aromatic functional groups at each remaining stem domain. Namely, the artificial groups played a prosthetic role to recover the function of the proteins. This strategy may contribute to the development of a novel approach for protein engineering, and may inspire an innovative design concept of protein-based biomaterials and biodevices.

Results and discussion

Construction of the stem-truncated mutants (STM1–6)

We constructed expression vectors for six stem-truncated mutants of Hla (STM1–6) (Figure 1a), to investigate the dependency of Hla hemolytic activity on the length of the stem domain. STM1 had a stem domain with the same length as that of the wild-type Hla, whereas four, six, 18, 14, and 24 amino acid residues were deleted from the central stem domain of Hla in a stepwise fashion using genetic engineering methodology for STM2, STM3, STM4, STM5, and STM6, respectively.

In all mutants, four amino acid residues located at the β-turn structure of the stem domain were replaced with the sequence Cys-Pro-Asp-Gly, which allows site-specific chemical modification via a cysteine-selective reaction while retaining the β-turn structure of the loop.[22] No endogenous cysteine remained in Hla, thereby allowing chemical modification specifically at the tip of the stem domain of Hla mutants. A molecular modeling study of the mutants using the PyMOL molecular graphics system (http://www. pymol. org) estimated that the length of the truncated stem regions was ca. 8, 11, 13, 22, and 35 Å for STM2, STM3, STM4, STM5, and STM6, respectively (Figure 1b). These six stem-truncated mutants were prepared from *E. coli* BL21(DE3) bacterial cell lysates, and were purified to homogeneity by nickel chelate affinity chromatography, followed by size-exclusion chromatography. To prevent the aggregation of each mutant, we used a buffer containing 200 mM arginine hydrochloride in all purification and measurement processes.[23–26]

Wild-type Hla exists as a monomeric form in an aqueous buffer solution in the absence of lipid membranes or detergents. Similarly, the size-exclusion chromatography of STM1 revealed that it adopted a monomeric form in Tris-HCl buffer (pH 8.0; 50 mM, containing 200 mM NaCl, 200 mM arginine hydrochloride, and 5 mM dithiothreitol) (Figure S1, Supporting Information). Regarding STM2, the chromatogram suggested the presence of multimeric assemblies, possibly corresponding to 14-meric and 7-meric forms, in addition to the monomeric form under the same conditions. Moreover, STM3–6 are likely to exist as 14-meric forms with a small quantity of 7-meric forms. In fact, the analysis of STM6 in the same buffer via size-exclusion chromatography with a multiangle light scattering (SEC-MALS) detector suggested that the oligomeric species contained 14-meric and 7-meric forms (Figure S2, Supporting Information). These observations are consistent with those of a previous report,[27] *i.e.*, the stem domain played a crucial role in preventing spontaneous assembling of Hla in the absence of membranes. The wild-type Hla 7-mer, once formed, is able to

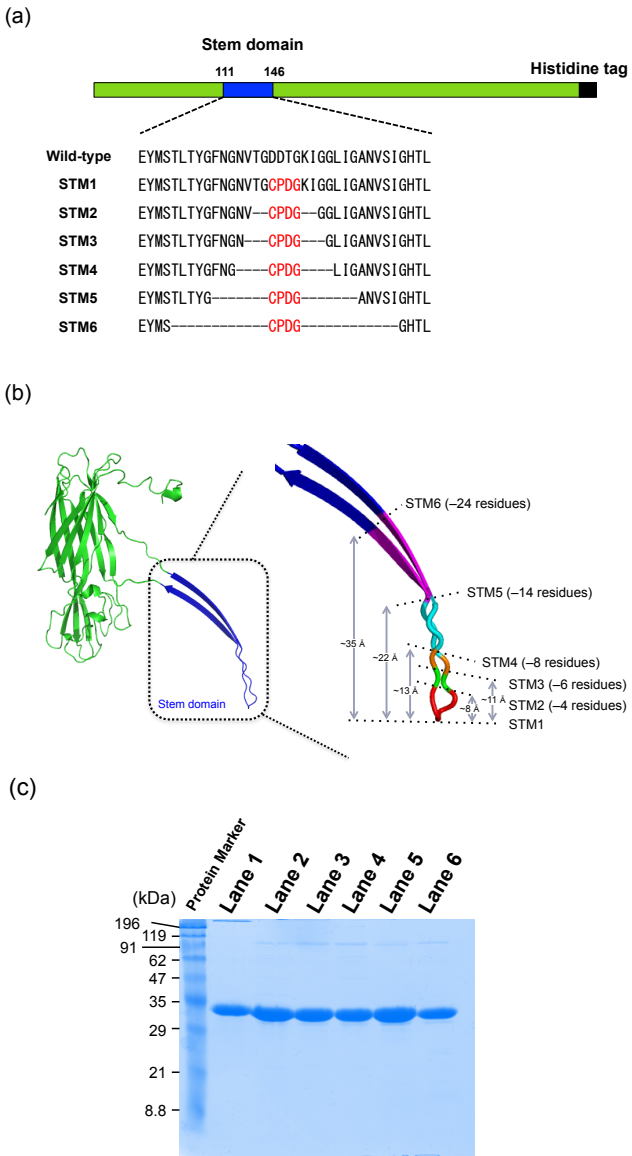

Figure 1. (a) Schematic image of wild-type α-hemolysin (Hla) and its six stem-truncated mutants (STM1–6), consisting of a stem domain (blue), a histidine tag (black), and other regions (green). (b) The crystal structure of the monomeric part in a 7-meric assembly of wild-type Hla (left), and a magnified structure of its stem domain (right). The length of the truncated region of each mutant was evaluated using the PyMOL program. (c) SDS–PAGE of the stem-truncated mutants of Hla: monomeric form of STM1 (lane 1), and 14-meric form of STM2 (lane 2), STM3 (lane 3), STM4 (lane 4), STM5 (lane 5), and STM6 (lane 6).

tolerate sodium dodecyl sulfate (SDS) and appears as a band around 200 kDa on SDS–PAGE.[28,29] In contrast, the stem-truncated mutants STM2–6 appeared as monomers in SDS gels, indicating that their oligomeric assemblies are able to dissociate into monomers in the presence of a strong surfactant (Figure 1c).

Hemolytic activities of the stem-truncated mutants

The hemolytic activities of the six stem-truncated mutants were evaluated by adding monomeric (STM1) and 14-meric (STM2–6; 45 μM) forms of each mutant, respectively, to a suspension

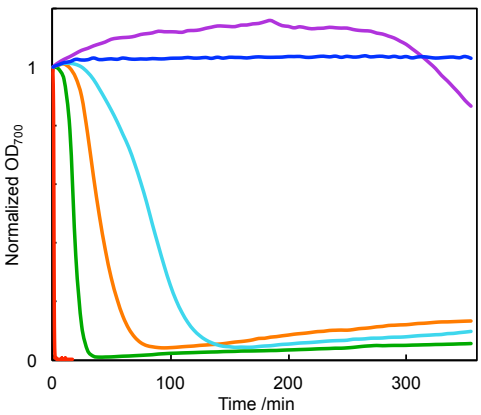

Figure 2. Time-course curves of the hemolysis of sheep red blood cells (SRBCs) by STM1 (red), STM2 (green), STM3 (orange), STM4 (cyan), STM5 (purple), and STM6 (blue) (each, 0.02 mg/mL) in PBS buffer solution (pH 7.4, containing 200 mM arginine hydrochloride) at 25 °C, as monitored by optional density at 700 nm.

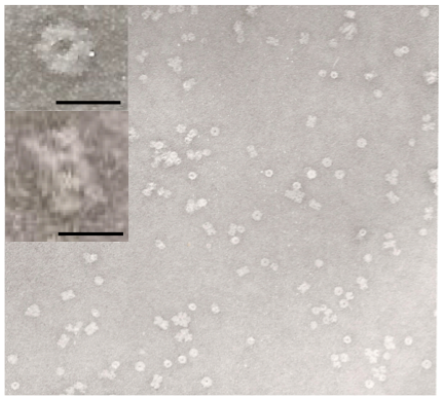

Figure 3. Transmission electron micrograph (negative staining with uranyl acetate) of STM5 in Tris-HCl buffer (pH 8.0; 50 mM, containing 200 mM NaCl and 200 mM arginine hydrochloride). Scale bars, 10 nm.

of sheep red blood cells (SRBCs) in PBS buffer (pH 7.4, containing 200 mM arginine hydrochloride) at 25 °C, where the progress of hemolysis was monitored by optical density at 700 nm (OD_{700}).[30] STM1, which has the longest stem domain, caused complete hemolysis immediately. Importantly, although STM2–6 can exist as a 14-meric form in the buffer solution, most of them exhibited hemolytic activities, and the rates of hemolysis were deeply dependent on the length of the stem domain (Figure 2). Namely, the mutant that possessed a shorter stem domain tended to show a slower hemolysis profile toward SRBCs compared with those that possessed longer stem domains. Actually, STM2 led to complete hemolysis within 30 min. In contrast, STM6, which had the shortest stem domain, hardly exhibited any hemolytic activity, as practically no hemolysis was observed even after overnight incubation at 25 °C. STM5 also exhibited a quite low activity, whereas STM2–4 had moderate activities with a clear dependence on the length of the remaining stem domain.

Hemolytic activity of STM5 oligomers

Among the stem-truncated mutants described above, we focused on STM5, which mostly lost hemolytic activity. Importantly, when the mixture of SRBCs and the 14-meric form of STM5 in PBS buffer (pH 7.4, containing 200 mM arginine hydrochloride) was incubated for 30 min at 25 °C, followed by washing out with the same buffer three times, the western blot analysis of the resulting sample displayed the presence of STM5 (Figure S3, Supporting Information). This observation means that STM5, although it had mostly lost the stem domain, preserved the ability to attach to SRBCs. This was also likely the case with STM6 (Figure S3, Supporting Information).

As mentioned above, size-exclusion chromatography of STM5 showed the formation of the 14-meric form, with a small quantity of the 7-meric form. The equilibrium between the 14-meric and 7-meric forms was considered to be very slow, as the two species could be separated by multicycle purification using size-exclusion chromatography. A transmission electron micrograph (TEM) of STM5 observed by negative staining with uranyl acetate displayed doughnut-like assemblies consisting of seven monomeric units and double-barreled assemblies likely derived from face-to-face dimerization of the 7-meric form (Figure 3). The TEM image also showed tube-like structures corresponding to the side view of the 14-meric form of STM5. It is likely that the hydrophobic interaction between the remaining stem domains encouraged the formation of the oligomeric assemblies.

The comparison of the hemolytic activity of STM5 in the 14-meric form with that observed in the 7-meric form revealed that these oligomeric species had almost the same activity toward SRBCs at 25 °C (Figure S4, Supporting Information). Sodium deoxycholate encourages the 7-meric ring formation of wild-type Hla monomer[31] and stabilizes its transmembrane region, the "β-barrel pore." The addition of 6.25 mM sodium deoxycholate to the Tris-HCl buffer solution of the 14-meric form resulted in the formation of the 7-meric form, as observed by TEM (Figure S5, Supporting Information).

Electron paramagnetic resonance (EPR) spectroscopy of STM5 labeled with sulfhydryl-specific nitroxide (1-oxyl-2,2,5,5-tetramethyl-Δ3-pyrroline-3-methyl) methanethiosulfonate (MTSL) at the cysteine residue in the stem domain also suggested the transition of the 14-meric form into the 7-meric form upon attachment to SRBCs or in the presence of 6.25 mM sodium deoxycholate (Figure S6A, Supporting Information). The EPR spectrum of the PBS buffer solution (pH 7.4, containing 200 mM arginine hydrochloride) containing the 14-meric form of spin-labeled STM5 gave the broadened component in addition to that of the corresponding 7-meric form observed in the same buffer solution. As the molecular motion can be expected to be more restricted in the 14-meric form than in the 7-meric form, we tentatively assigned the component to the 14-meric form of spin-labeled STM5 (Figure S6B, Supporting Information). In contrast, the EPR spectra of the 14-meric and 7-meric forms in PBS buffer (pH 7.4; containing 6.25 mM sodium deoxycholate) mostly overlapped with each other, indicating that the 14-meric form component was diminished in the spectrum. Similarly, in the suspension of SRBCs, the 14-meric and 7-meric forms also showed substantially the same spectra. These results are consistent with the abovementioned transition of the 14-meric form into the 7-meric form observed by TEM in the presence of sodium deoxycholate or SRBCs.

It should be noted here that the EPR spectrum of the STM2 monomer displayed sharp signals, as shown in Figure S7 (see Supporting Information). In addition, the EPR spectra of the 14-meric and 7-meric forms of STM5 shown in Figure S6 also displayed the presence of sharp signals, together with broad ones assigned to the 14- and 7-meric forms. These spectral profiles suggest the existence of the monomeric form of STM5 in the timescale of EPR spectroscopy, whereas chromatography showed no peak corresponding to the monomeric form for the purified 14-meric and 7-meric forms of STM5. These results suggest that there is a significantly slow equilibrium among the 14-, 7-, and monomeric forms of STM5 in the presence of sodium deoxycholate or SRBCs.

The effects of the chemically engineered stem domain of STM5 on hemolytic activity

The stem domain of STM5 is 14 amino acid residues shorter than that of wild-type Hla. The weak hemolytic activity of STM5 is likely due to the short stem domain, which could not penetrate through the cell membrane of SRBCs. Interestingly, we found that the hemolytic activity of STM5 was significantly recovered by introducing synthetic units at the tip of its shortened stem domain, to compensate for the missing residues. In fact, three maleimide derivatives bearing phenyl, pyrenyl, and fluoresceinyl groups (PhM, PyM, and FlM, respectively; see Figure 4) were introduced via Michael-type addition between the thiol group of the genetically introduced cysteine residue and the maleimide group. Hemolytic activity was evaluated by adding this chemically modified STM5 (45 μM) to a suspension of SRBCs in PBS buffer (pH 7.4, containing 200 mM arginine hydrochloride) at 25 °C. After the resulting mixture was incubated for 30 min and then washed with the buffer three times, a western blot analysis clearly displayed the bands corresponding to STM5, STM5-PhM, STM5-PyM, and STM5-FlM, respectively (Figure S8, Supporting Information). This indicates that the binding ability of STM5 to the membrane is preserved even after the chemical modification of its remaining stem domain with synthetic functional moieties. Interestingly, STM5 modified with PyM (STM5-PyM) clearly showed recovery of the hemolytic activity of STM5 (Figure 5a and 5b). Although STM5 modified with PhM (STM5-PhM) showed much lower hemolytic activity than did STM5-PyM, it was still higher than that of STM5 (Figure 5c). In contrast, STM5 modified with FlM (STM5-FlM) hardly showed any hemolytic activity (Figure 5d). Thus, the hemolytic activity of modified STM5 was highly dependent on the functional group that was introduced at its remaining stem domain, in which both the length and polarity of the molecular unit are likely to be important factors.

Matile *et al*. reported that the rigid-rod molecules carrying a shorter hydrophobic region compared with the host lipid bilayers showed low ion-transport activities.[32] Based on the mattress model proposed by Mouritsen and Bloom in 1984,[33] it is likely that the low hemolytic activity of STM5 without modification is caused by the deformation of the SRBC membrane to compensate for the unfavorable hydrophobic interactions with the immature pore of STM5, whereas the PyM moiety of STM5-PyM would be able to contribute to the "hydrophobic matching." It is noteworthy that the location of the PyM moiety on the stem-truncated mutant is crucial for the successful recovery of hemolytic activity. In fact, we prepared a stem-truncated mutant bearing a cysteine reside at the cap domain (K46C) based on the known stem-truncated Hla

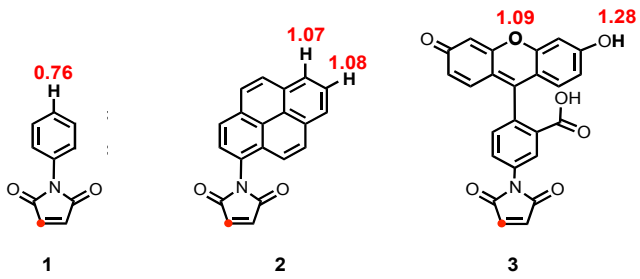

Figure 4. Chemical structure of three maleimide derivatives (1–3). **1**, *N*-Phenylmaleimide (PhM); **2**, *N*-(1-pyrenyl)maleimide (PyM); **3**, fluorescein-5-maleimide (FlM). The longest distances (nm) between the carbon atoms marked with a red dot and the hydrogen or oxygen atoms in the aromatic group of each molecule are shown in red. The distances were evaluated from the structures optimized by a molecular mechanics calculation with an MMFF force field using Spartan'08.

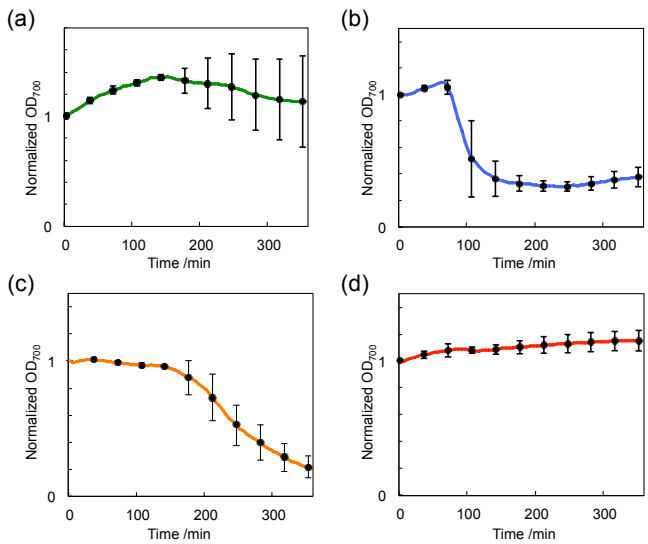

Figure 5. Time-course curves of the hemolysis of SRBCs by (a) STM5, (b) STM5-PyM, (c) STM5-PhM, and (d) STM5-FlM (each, 0.2 mg/mL) in PBS buffer (pH 7.4, containing 200 mM arginine hydrochloride) at 25 °C, as monitored by optical density at 700 nm (OD_{700}). OD_{700} was measured every 5 min. Data are means ± standard deviations (every 35 min for clarity) of three independent experiments.

mutant.[27] The PyM-appended protein prepared from this mutant did not cause the hemolysis of SRBCs (Figure S9, Supporting Information).

To investigate the ion permeability of STM5-PyM at the membrane, we performed conductivity measurements for the planar lipid bilayers that contained STM5, STM5-PyM, and STM5-FlM (Figure S10, Supporting Information), respectively, which were prepared by dropping the solutions of the proteins on each membrane formed between two chambers containing HEPES buffer (pH 7.0; 10 mM, containing 100 mM KCl). In the case of the membrane containing STM5, as was expected from its low hemolytic activity, the increase in the current was considerably slow, and only an irreversible one-step increase in the current was observed within a period of 35 s. In contrast, in the case of the membrane containing STM5-PyM, a distinct increase in the current was observed within the same time range. Although the observed current profile showed fluctuation,

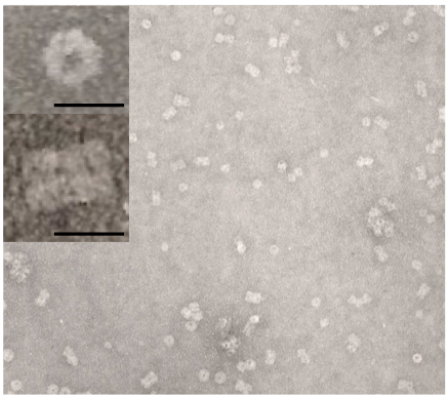

Figure 6. Transmission electron micrograph (negative staining with uranyl acetate) of STM5-PyM in Tris-HCl buffer (pH 8.0; 50 mM, containing 200 mM NaCl and 200 mM arginine hydrochloride). Scale bars, 10 nm.

unlike wild-type Hla,[34–37] a stepwise increase (2 pA) in the current was clearly displayed (inset figures, Supporting Information), indicating that the formation of a channel in a lipid membrane contributes to the hemolytic activity of STM5-PyM. Therefore, the PyM moiety likely compensated for the shortened stem domain of STM5, to improve ion-transport activity across the membrane. The dynamic feature of the profile is possibly caused by the rather flexible conformation around the PyM units, to form a supramolecular pore in the lipid membrane.[38–40] In contrast, membranes including STM5-FlM displayed no conductivity under the same condition. Unlike the cases of STM5-PhM and STM5-PyM, STM5-FlM showed neither hemolytic activity nor produced current in the conductivity measurement. One plausible explanation for this finding is that the fluorescein unit is anionic and more polar than the phenyl and pyrenyl groups, and might slip inside the remaining β-barrel pore with a hydrophilic inner surface,[41] so as to block the flow of ions through the membrane.

Similar to STM5 without modification, STM5-PyM likely adopts a 14-meric form in Tris-HCl buffer (pH 8.0; 50 mM, containing 200 mM NaCl and 200 mM arginine hydrochloride), as suggested by TEM (Figure 6). The UV absorption spectrum of STM5-PyM showed an absorption band around 350 nm, whereas its fluorescence spectrum showed emission bands at around 400 nm and 470 nm, suggesting the formation of an excimer of the pyrene units (Figure S11a, b, Supporting Information). In contrast, in Tris-HCl buffer containing 6.25 mM sodium deoxycholate, the UV spectrum of STM5-PyM showed a relatively sharp peak at around 350 nm, and the fluorescence emission at 400 nm was intensified together with a slight decrease in the intensity at 470 nm, corresponding to the excimer. These spectral profiles suggest that the pyrene units of STM5-PyM are in close proximity to each other in the 14-meric form in an aqueous buffer solution, whereas they become separated after transition into the 7-meric form in the solution containing 6.25 mM sodium deoxycholate and also in the lipid bilayers. Here it should be noted that the UV spectrum of STM5-PyM with deoxycholate still showed the weak emission at 470 nm suggesting that the assembly of pyrene units possibly allows for formation of the pore in the membrane.

We also attempted the chemical modification of STM6 with PhM, PyM, and FlM, and obtained a similar tendency compared with STM5 regarding the restoration of hemolytic activity. Namely, the chemically modified STM6 bearing pyrenyl-maleimide exhibited partially restored hemolytic activity, whereas the fluorescein-maleimide-appended STM6 did not show such effects (Figure S12, Supporting Information). However, in all cases, the restored hemolytic activities of these chemically modified mutants were lower than those of the corresponding STM5 derivatives.

Conclusions

We demonstrated the construction of semibiological protein pores based on the stem-truncated mutant of Hla, STM5, via chemical modification with synthetic moieties that compensated for the lost transmembrane stem domain. The hydrophobic phenyl-maleimide unit worked as an elongated stem domain of STM5 and contributed moderately to the recovery of hemolytic activity. The pyrenyl-maleimide unit, which had a larger hydrophobic surface, allowed more efficient recovery of the hemolytic activity of STM5. In contrast, the hydrophilic fluorescein-maleimide unit hardly showed any recovery of the hemolytic activity of STM5. These results indicate that the hemolytic activity of Hla could be effectively modulated by the properties of the synthetic unit attached to the tip of the truncated stem domain. Although the present work is a proof-of-concept study, our approach to the engineering of proteins may not only contribute to the development of highly regulated nanopore devices, but also inspire innovative ideas for protein-based hybrid materials.

Materials and methods

Construction of the expression vectors for wild-type Hla and stem-truncated mutants (STM1–6)

A DNA fragment encoding staphylococcal α-hemolysin without the signal sequence was amplified using KOD-Plus DNA polymerase (TOYOBO, Osaka, Japan) using *S. aureus* strain Mu50 (ATCC 700699) genomic DNA as the template and the following primers: α-hemolysin-S (5′–CATGCCATGGCAGATTCTGATATTAATATTAAAACCGG–3′), α-hemolysin-AS (5′–CCGCTCGAGATTTGTCATTTCTTCTTTTTCCCAATCG–3′) The PCR products were inserted into the NcoI and XhoI sites of the pET28b vector (Merck, Whitehouse Station, NJ). A His6 tag was fused at the C terminus for purification by nickel chelate affinity chromatography. The expression vectors for the stem-truncated mutants (STM1–6) were constructed using the KOD-Plus-Mutagenesis Kit (TOYOBO). The DNA fragments encoding the stem domain of Hla were removed and replaced with the sequence TGCCCGGATGGN (Cys-Pro-Asp-Gly) using KOD-Plus DNA polymerase and the following primers:

STM1-S: 5′–TGCCCGGATGGAAAAATTGGCGGCCTTA–3′, STM1-AS: 5′–ACCAGTAACATTACCGTTGAATCC–3′,
STM2-S: 5′–TGCCCGGATGGTGGCGGCCTTATTGGTGCAA–3′
STM2-AS: 5′–AACATTACCGTTGAATCCATAAGTTAAAG–3′,
STM3-S: 5'–TGCCCGGATGGCGGCCTTATTGGTGCAAATGTTTC–3′,
STM3-AS: 5′–ATTACCGTTGAATCCATAAGTTAAAGTACT–3′,

STM4-S: 5′–TGCCCGGATGGCCTTATTGGTGCAAATGTTTC–3′,
STM4-AS: 5'–ACCGTTGAATCCATAAGTTAAAGTACT–3′,
STM5-S: 5′–TGCCCGGATGGTGCAAATGTTTCGATTGGTC–3′,
STM5-AS: 5′–TCCATAAGTTAAAGTACTCATATACTCTTTTGT–3′,
STM6-S: 5′–TGCCCGGATGGCATTGGTCATACAATGAAATAT–3′,
STM6-AS: 5′–TAAAGTACTCATATACTCTTTTGTATCAATCG–3′.

Expression and purification of STM1–6

Escherichia coli BL21(DE3) transformed with the expression vector were grown at 28 °C in 2× YT medium containing 16 g/L of tryptone, 10 g/L of yeast extract, 5 g/L of NaCl, and 30 mg/L of kanamycin. After growing the culture to an optical density of 0.7 at 600 nm, IPTG (final concentration, 500 μM) was added to the culture to induce expression of the protein. Subsequently, the culture was incubated overnight and centrifuged at 7000 rpm for 15 min at 4 °C. After removal of the supernatant, the resulting pellet was suspended in Tris-HCl buffer (pH 8.0; 50 mM, containing 200 mM NaCl, 200 mM arginine hydrochloride, and 5 mM dithiothreitol; 50 mL for 1 L of culture). The resulting cell suspension was sonicated for 20 min on ice and then centrifuged at 40,000 × *g* for 30 min at 4 °C. The supernatant was loaded onto 1 mL of resin (Ni Sepharose 6 Fast Flow, GE Healthcare), which was then washed with 20 mL of Tris-HCl buffer (pH 8.0; 50 mM, containing 5 mM imidazole, 200 mM NaCl, 200 mM arginine hydrochloride, and 5 mM dithiothreitol). The proteins were eluted with 10 mL of Tris-HCl buffer (pH 8.0; 50 mM, containing 250 mM imidazole, 200 mM NaCl, 200 mM arginine hydrochloride, and 5 mM dithiothreitol) at 4 °C. Fractions containing the protein were collected, dialyzed against Tris-HCl buffer (pH 8.0; 50 mM, containing 200 mM NaCl, 200 mM arginine hydrochloride, and 5 mM dithiothreitol) for more than 4 h at 4 °C, and then further purified by size-exclusion chromatography (HiLoad™ 26/60 Superdex 200-pg, GE Healthcare). The purity and homogeneity of the proteins were evaluated using sodium dodecyl sulfate polyacrylamide gel electrophoresis (SDS–PAGE).

Chemical modification

After the removal of dithiothreitol with a PD-10 desalting column (GE Healthcare), a DMF solution of *N*-phenylmaleimide (Tokyo Chemical Industry, Tokyo, Japan), *N*-(1-pyrenyl) maleimide (Tokyo Chemical Industry, Tokyo, Japan), or fluorescein-5-maleimide (Santa Cruz Biotechnology, Santa Cruz, CA, USA) (each, 20-fold molar excess) was added to a phosphate-buffered saline (PBS, pH 7.4, including 200 mM arginine hydrochloride solution of STM5; 3 mg/mL), and the resulting mixture was stirred overnight under an Ar gas atmosphere at 4 °C. The reaction mixture was centrifuged at 40,000 × *g* for 30 min at 4 °C, and the supernatant was filtered to remove insoluble substances. The filtrate was then subjected to size-exclusion chromatography (HiLoad™ 26/60 Superdex 200-pg, GE Healthcare) to allow the isolation of chemically modified STM5. The unreacted free thiol groups in this chemically modified STM5 were evaluated by Ellman's assay.

Hemolytic activity assays

Preserved blood collected from sheep (Nippon Biotest Laboratories Inc., Tokyo, Japan) was centrifuged at 1,500 × *g* for 5 min at 4 °C and washed several times with PBS buffer (pH 7.4, containing 200 mM arginine hydrochloride). The erythrocytes were then suspended in PBS buffer (pH 7.4, containing 200 mM arginine hydrochloride), so that the resulting mixture had a turbidity of 0.5 O.D. at 700 nm with a volume of 2.95 mL. The resulting suspension was incubated for 1 h at 25 °C. A Tris-HCl buffer (pH 8.0; 50 mM, containing 200 mM arginine hydrochloride) or PBS buffer solution (pH 7.4, containing 200 mM arginine hydrochloride) of protein (50 μL) was added to the erythrocyte suspension thus prepared and the activity was evaluated by measuring the turbidity at 700 nm at 25 °C.

Western blot analysis of proteins that bound to SRBCs

The binding of proteins to sheep red blood cells (SRBCs) was evaluated by western blot analysis. Each protein (0.2 mg/mL) was incubated with SRBCs (50 μL, OD_{700} = 0.5) in PBS buffer (pH 7.4, containing 200 mM arginine hydrochloride) for a definite period at 25 °C. Subsequently, the supernatant and pellet fractions were separated by centrifugation at 1,500 × *g* for 5 min, and the collected pellets were washed with 500 μL of the same buffer three times. The pellets were then dissolved in buffer containing 1.4% (w/v) SDS and the resulting mixture was subjected to SDS–PAGE on a 15% gel. The gel was electrotransferred onto a nitrocellulose membrane (GE Healthcare). To detect the His_6-tag of proteins, the membrane was incubated with 15 mL of 100 ng/mL of a horseradish peroxidase (HRP)-conjugated anti-His antibody (Santa Cruz Biotechnology) at room temperature for 30 min after blocking with Blocking One (50 mL; Nacalai Tesque, Kyoto, Japan), and then washed three times with a washing solution (PBS buffer containing 0.1% Tween 20, PBS-T). The binding of proteins was visualized using Chemi-Lumi One L (Nacalai Tesque).

Transmission electron microscopy

An aliquot of a solution comprising the protein (0.1 mg/mL) in Tris-HCl buffer (pH 8.0; 50 mM, containing 200 mM NaCl and 200 mM arginine hydrochloride) was mounted on a Cu300 grid with a carbon-coated parlodion film, and the grid was washed with the same buffer that was used for the sample. After drying with pre-water-soaked filter paper, the grid was negatively stained with 2% uranyl acetate for 10 min. TEM micrographs were then recorded on a JEM1010 (JEOL, Japan) transmission electron microscope operating at an anode voltage of 80 kV with a Fuji FG electron image film (11.8 × 8.2 cm, Fujifilm, Japan).[42]

Site-directed spin labeling and EPR spectroscopy

A nitroxide paramagnetic spin label was introduced at the end of the remaining stem domain (β-turn) of STM5 by site-specific reaction of the cysteine residue with (1-oxyl-2,2,5,5-tetramethyl-Δ3-pyrroline-3-methyl) methanethiosulfonate (MTSL; Toronto Research Chemicals Inc., North York, Canada). After purification by nickel affinity chromatography, STM5 was incubated with 10 mM DTT for 30 min at room temperature, and the buffer of the resulting solution was changed to PBS buffer (pH 7.4, containing 200 mM arginine hydrochloride) on a PD-10 desalting column (GE Healthcare).

MTSL (10 eq. to STM5) was added immediately to the resulting solution, and the mixture was stirred overnight at 4 °C. The reaction solution was subjected to size-exclusion chromatography (HiLoad™ 26/60 Superdex 200-pg, GE Healthcare). The EPR spectra were recorded on a Bruker ELEXSIS E580 EPR spectrometer at room temperature.

Conductance measurement

Ion-channel current recordings were performed as follows. A planar lipid bilayer was prepared using a reported procedure.[43,44] A major–minor lipid mix[45] in *n*-decane was painted onto an orifice (d = 150 μm) that was sandwiched by two chambers containing HEPES buffer (pH 7.0; 10 mM, containing 100 mM KCl, 0.30 mL each). A PBS buffer solution of the protein (13 mg/mL, pH 7.4, containing 200 mM arginine hydrochloride) was 10-fold diluted with the HEPES buffer (pH 7.0; 10 mM, containing 100 mM KCl), and the resulting mixture was added drop-wise to the upper chamber using a glass pipette (total, ~300 μL). Current was measured with a CEZ2400 amplifier (Nihon Kohden, Tokyo, Japan) and stored on a computer using a Power Lab (AD Instruments, Nagoya, Japan) at a 40 kHz sampling rate. Recordings were filtered at 1 kHz. To monitor the channel current, membrane voltage was applied at 50 mV. All the current recordings were performed at 20 °C. The single-channel *I–V* profile was obtained by plotting the single-channel current I as a function of membrane potential *V*.

Acknowledgments

We thank Dr. Yoshikazu Tanaka for kindly providing the expression vectors for staphylococcal α-hemolysin. This work was partially supported by the Ministry of Education, Science, Sports and Culture, Japan, Grants-in-Aid for Young Scientists and Scientific Research on Innovative Areas "Spying minority in biological phenomena (No.3306)" (23115003), and by Management Expenses Grants for National Universities Corporations from the Ministry of Education, Culture, Sports, Science and Technology of Japan (MEXT) to K.K.

Notes and references

[a] Institute of Multidisciplinary Research for Advanced Materials, Tohoku University, 2-1-1, Katahira, Aoba-ku, Sendai 980-8577, Japan. E-mail: kinbara@tagen.tohoku.ac.jp

[b] Department of Medical Genome Sciences, Graduate School of Engineering, The University of Tokyo, 5-1-5 Kashiwanoha, Kashiwa 277-8562, Japan.

[c] Institute of Medical Science, The University of Tokyo, 4-6-1 Shirokanedai, Minato-ku, Tokyo 108-8639, Japan.

[d] Department of Bioengineering and Department of Chemistry and Biotechnology, School of Engineering, The University of Tokyo, 7-3-1, Hongo, Bunkyo-ku, Tokyo 113-8656, Japan.

[e] Department of Applied Chemistry, School of Engineering, The University of Tokyo, 7-3-1, Hongo, Bunkyo-ku, Tokyo 113-8656, Japan.

† Electronic Supplementary Information (ESI) available: [size-exclusion chromatography and activity assay of Hla mutants, SDS-PAGE and Western blot analysis, TEM images, EPR spectra, Conductance measurements, Absorption, fluorescence, and CD spectra.]. See DOI: 10.1039/b000000x/

1. T. L. Foley, M. D. Burkart, *Curr. Opin. Chem. Biol.*, 2007, **11**, 12-19.
2. I. S. Carrico, *Chem. Soc. Rev.*, 2008, **37**, 1423-1431.
3. D. P. Gamblin, S. I. van Kasteren, J. M. Chalker, B. G. Davis, *FEBS J.*, 2008, **275**, 1949-1959.
4. Y. Yoshioka, S.-I. Tsunoda, Y. Tsutsumi, *Chem. Cent. J.*, 2011, **5**, 25.
5. M. E. B. Smith, F. F. Schumacher, C. P. Ryan, L. M. Tedaldi, D. Papaioannou, G. Waksman, S. Caddick, J. R. Baker, *J. Am. Chem. Soc.*, 2010, **132**, 1960-1965.
6. J. M. Chalker, G. J. L. Bernardes, Y. A. Lin, B. G. Davis, *Chem. Asian J.*, 2009, **4**, 630-640.
7. X. Chen, K. Muthoosamy, A. Pfisterer, B. Neumann, T. Weil, *Bioconjug. Chem.*, 2012, **23**, 500-508.
8. J. A. Prescher, C. R. Bertozzi, *Nat. Chem. Biol.*, 2005, **1**, 13-21.
9. S. Lepthien, L. Merkel, N. Budisa, *Angew. Chem. Int. Ed. Engl.*, 2010, **49**, 5446-5450.
10. D. Ishii, K. Kinbara, Y. Ishida, N. Ishii, M. Okochi, M. Yohda, T. Aida, *Nature*, 2003, **423**, 628-632.
11. S. Muramatsu, K. Kinbara, H. Taguchi, N. Ishii, T. Aida, *J. Am. Chem. Soc.*, 2006, **128**, 3764-3769.
12. M. R. Banghart, M. Volgraf, D. Trauner, *Biochemistry*, 2006, **45**, 15129-15141.
13. P. Gorostiza, E. Isacoff, *Mol. Biosyst.*, 2007, **3**, 686-704.
14. S. Biswas, K. Kinbara, N. Oya, N. Ishii, H. Taguchi, T. Aida, *J. Am. Chem. Soc.*, 2009, **131**, 7556-7557.
15. S. Biswas, K. Kinbara, T. Niwa, H. Taguchi, N. Ishii, S. Watanabe, K. Miyata, K. Kataoka, T. Aida, *Nat. Chem.*, 2013, **5**, 613-620.
16. A. Lopez-Rodriguez, M. Holmgren, *PLoS One.*, 2012, **7**, e47693.
17. E. J. Gouaux, *Struct. Biol.*, 1998, **121**, 110-122.
18. G. Menestrina, M. D. Serra, G. Prévost, *Toxicon*, 2001, **39**, 1661-1672.
19. M. Montoya, E. Gouaux, *Biochim. Biophys. Acta*, 2003, **1609**, 19-27.
20. M. Rhee, M. Burns, *a Trends Biotechnol.*, 2006, **24**, 580-586.
21. S. Majd, E. C. Yusko, Y. N. Billeh, M. X. Macrae, J. Yang, M. Mayer, *Curr. Opin. Biotechnol.*, 2010, **21**, 439-476.
22. E. G. Hutchinson, J. M. Thornton, *Protein Sci*., 1994, **3**, 2207-2216.
23. K. Tsumoto, M. Umetsu, I. Kumagai, D. Ejima, J.S. Philo, T. Arakawa, *Biotechnol Prog.*, 2004, **20**, 1301-1308.
24. K. Tsumoto, D. Ejima, Y. Kita, T. Arakawa, *Protein Pept Lett.*, 2005, **12**, 613-619.
25. D. Ejima, R. Yumioka, T. Arakawa, K. Tsumoto, *J. Chromatogr. A*, 2005, **1094**, 49-55.
26. T. Arakawa, D. Ejima, K. Tsumoto, N. Obeyama, Y. Tanaka, Y. Kita, S. N. Timasheff, *Biophys. Chem.*, 2007, **127**, 1-8.
27. Spontaneous oligomerization of the stem-truncated mutant of Hla has been reported (S. Cheley, M. S. Malghani, L. Song, M. Hobaugh, J. E. Gouaux, J. Yang, H. Bayley, *Protein Eng.*, 1997, **10**, 1433-1443.). The mutant in this report has almost the same length of the stem domain with STM6.
28. D. M. Czajkowsky, S. Sheng, Z. Shao, *J. Mol. Biol.*, 1998, **276**, 325-330.

29. G. Maglia, M. Henricus, R. Wyss, Q. Li, S. Cheley, H. Bayley, *Nano Lett.*, 2009, **9**, 3831-3836.
30. M. Ui, Y. Tanaka, Y. Araki, T. Wada, T. Takei, K. Tsumoto, S. Endo, K. Kinbara, *Chem. Commun. (Camb)*., 2012, **48**, 4737-4739.
31. S. Bhakdi, R. Fussle, J. Tranum-Jensen, *Proc. Natl. Acad. Sci.*, 1981, **78**, 5475-5479.
32. B. Ghebremariam, V. Sidorov, S. Matile, *Tetrahedron Lett.*, 1999, **40**, 1445-1448.
33. O. G. Mouritsen, M. Bloom, *Biophys. J.*, 1984, **46**, 141-153.
34. G. Menestrina, *J. Membr. Biol.*, 1986, 90, 177-190.
35. O.V. Krasilnikov, P.G. Merzlyak, L.N. Yuldasheva, C.G. Rodrigues, S. Bhakdi, A. Valeva, *Mol. Microbiol.*, 2000, **37**, 1372-1378.
36. H. Suzuki, K.V. Tabata, H. Noji, S. Takeuchi, *Biosens. Bioelectron.*, 2007, **22**, 1111-1115.
37. R. Kawano, Y. Tsuji, K. Sato, T. Osaki, K. Kamiya, M. Hirano, T. Ide, N. Miki, S. Takeuchi, Sci. Rep., 2013, **3**, 1995.
38. T. Muraoka, T. Shima, T. Hamada, M. Morita, M. Takagi, K.V. Tabata, H. Noji, K. Kinbara, *J. Am. Chem. Soc.,* 2012, **134**, 19788-19794.
39. M. Jung, H. Kim, K. Baek, K. Kim, *Angew. Chem. Int. Ed.*, 2008, **47**, 5755-5757.
40. M. Boccalon, E. Iengo, P. Tecilla, *J. Am. Chem. Soc.,* 2012, **134**, 20310-20313.
41. G. Menestrina, M. D. Serra, G. Prévost, *Toxicon*, 2001, **39**, 1661-1672.
42. T. Takei, A. Okonogi, K. Tateno, A. Kimura, S. Kojima, K. Yazaki, K. Miura, *J. Biochem.*, 2006, **139**, 271-278.
43. T. Ide, T. Yanagida, *Biochem. Biophys. Res. Commun.*, 1999, **265**, 595-599.
44. K. V Tabata, K. Sato, T. Ide, T. Nishizaka, A. Nakano, H. Noji, *EMBO J.*, 2009, **28**, 3279-3289.
45. K. Matsuoka, L. Orci, M. Amherdt, S. Y. Bednarek, S. Hamamoto, R. Schekman, T. Yeung, *Cell*, 1998, **93**, 263-275.

